

Final NASA NCC3-794 Report, April 7, 2005
Coleen Pugh and Wayne Mattice, University of Akron

Homopolyrotaxanes and Homopolyrotaxane Networks of PEO

Personnel:

- 1) Mr. Andrew Soehnlén (partially supported; Pugh)
- 2) Dr. Kaitian Xu (fully supported; Pugh)
- 3) Dr. Carin Helfer (partially supported; Mattice)
- 4) Dr. Guoqiang Xu (partially supported; Mattice)
- 5) Dr. Sagar Rane (partially supported; Mattice)

Presentations:

- 1) C.A. Helfer, W.L. Mattice and C. Pugh, "Monte Carlo Simulation of Threading of Poly(ethylene oxide)," ACS National Meeting, Boston, August 2002.
- 2) C. Pugh, K. Xu and A. Soehnlén, "Synthesis, Isolation and Properties of Amphiphilic Macrocrown Ethers," UAkron Sponsor's Program, October 2002.
- 2) C. Pugh and K. Xu, "Synthesis of (Poly)rotaxanes that Lack an Enthalpic Driving Force for Threading," invited lecture, ACS National Meeting, New Orleans, March 2003.
- 3) C. Pugh and K. Xu, "Synthesis (Poly)Rotaxanes that Lack an Enthalpic Driving Force for Threading," invited lecture, 7th American German Polymer Symposium, Bayreuth, German, July 2003.
- 4) C. Wesdemiotis, K.M. Wollyung, C. Pugh and K. Xu, "Mass Spectrometry Studies of Polyrotaxanes," 16th International MS Conference, Edinburgh, Scotland, September 2003.
- 5) C. Pugh, K. Xu, C.A. Helfer, G. Xu, S.S. Rane and W.L. Mattice, "Synthesis of (Poly)rotaxanes that Lack an Enthalpic Driving Force for Threading", International Symposium on Polymer Chemistry (PC2004), Changchun, China, June 2004.

Publications

- 1) C.A. Helfer, W.L. Mattice and C. Pugh, "Monte Carlo Simulation of Threading of Poly(ethylene oxide)", *ACS PMSE Prepr.*, **87**, 334-335 (2002).
- 2) C. Pugh and K. Xu, "Synthesis of (Poly)rotaxanes that Lack an Enthalpic Driving Force for Threading", *ACS Polymer Prepr.*, **44**(1), 606-607 (2003).
- 3) C.A. Helfer, G. Xu, W.L. Mattice and C. Pugh, "Monte Carlo Simulations Investigating the Threading of Cyclic Poly(ethylene oxide) by Linear Chains in the Melt", *Macromolecules*, **36**, 10071-10078 (2003).
- 4) G. Xu, S.S. Rane, C.A. Helfer, W.L. Mattice and C. Pugh, "Monte Carlo Simulation of Solvent Effects on the Threading of Poly(ethylene oxide)," *Modeling Simul. Mater. Sci. Eng.*, **12**, S59-S71 (2004).
- 5) K.M. Wollyung, K. Xu, M. Cochran, A.M. Kasko, W.L. Mattice, C. Wesdemiotis and C. Pugh, "Synthesis and Mass Spectrometry Studies of an Amphiphilic Polyether-Based Rotaxane that Lacks an Enthalpic Driving Force for Threading", *Macromolecules*, **38**, 2574-2586 (2005).

Report

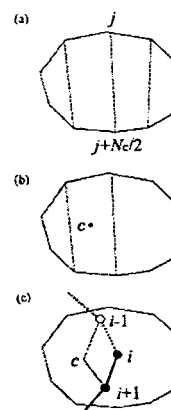
Table 1. Mean-Square Radii of Gyration ($\langle R_g^2 \rangle$), Principle Moments of the Radius of Gyration Tensor ($\langle L_1^2 \rangle$, $\langle L_2^2 \rangle$, $\langle L_3^2 \rangle$), and the Ratios of the Tensors of the Crown Ethers (Mass Fraction $X_c = 0.25$) in the Melt with $\text{CH}_3(\text{OCH}_2\text{CH}_2)_{13}\text{OCH}_3$ ($N_l = 21$).

Crown Ether	N_c beads	$\langle R_g^2 \rangle_{\text{cyclic}}$ (\AA^2)	$\langle L_1^2 \rangle$	$\langle L_2^2 \rangle$	$\langle L_3^2 \rangle$	$\langle L_2^2 \rangle / \langle L_1^2 \rangle$	$\langle L_3^2 \rangle / \langle L_1^2 \rangle$
24-C-8	12	13.5	8.03	4.42	1.02	0.55	0.13
30-C-10	15	18.5	12.2	5.10	1.30	0.42	0.11
42-C-14	21	27.7	18.3	7.11	2.27	0.39	0.12
60-C-21	30	41.1	27.0	10.4	3.70	0.39	0.14

373 K, and their extent of threading with PEO in the melt using coarse-grained Monte Carlo simulations on the 2nd (second nearest neighbor diamond) lattice,¹ which is a high coordination lattice whose coarse-grained chains can be reverse mapped into fully atomistic models in continuous space.^{2,3,4} Each bead consists of two backbone atoms (C-C or C-O), such that both 42-crown-14 (42-C-14) and linear $\text{CH}_3(\text{OCH}_2\text{CH}_2)_{13}\text{OCH}_3$ consist of 21 beads; C and O were treated equally in the long range interactions, and the short range interactions were based on the rotational isomeric state (RIS) model. The experimental density of the PEO melt at 373 K (1.06 g/mL) was achieved with occupancy of 21% of the lattice sites. We generally used a periodic box with 20 lattice steps on each side. Table 1 summarizes the equilibrated $\langle R_g^2 \rangle$ and principal moments of the R_g tensor ($\langle L_1^2 \rangle$, $\langle L_2^2 \rangle$, $\langle L_3^2 \rangle$) for four ring sizes. The ratio $\langle L_3^2 \rangle / \langle L_1^2 \rangle$ will approach zero if the rings are planar, and if so, the rings will have a circular shape if the ratio $\langle L_2^2 \rangle / \langle L_1^2 \rangle$ is also near one. The values of $\langle L_3^2 \rangle / \langle L_1^2 \rangle$ in Table 1 are slightly larger than zero, and those of $\langle L_2^2 \rangle / \langle L_1^2 \rangle$ are less than one, which indicates that these macrocrown ethers have ellipsoidal shapes that deviate from planarity, but can be represented by a series of planes. The threading events were therefore counted by first separating the macrocycles into a series of planes as illustrated in Scheme 1, in which the lines defining those planes were separated by no more than two beads. After identifying the center (c) of each plane, the bead (i) closest to the center of any linear chain within each plane was identified. If the beads $i-1$ and $i+1$ of the linear chain were located on opposite sides of the local plane, it was counted as a threading event. Figure 1a presents the extent of threading in the melt as

a function of the size of the rings (N_c) for a system consisting of 25% cycles using a 21-bead linear PEO chain ($N_l = 21$). Figure 1a shows that the extent of threading in the melt increases with increasing ring size, but is negligible (<1%) for rings with less than 30 atoms; the increase is much slower above 42-C-14, and the 60-crown-21 rings have the disadvantage that they undergo a significant amount of multiple threading events involving 2 to 3 linear chains.¹ Since 42-C-14 is approximately the optimum ring size for maximum spontaneous threading with inconsequential multiple threading, we concentrated both our synthetic and simulation studies on this ring size. Figure 1b presents the extent of threading of 42-C-14 with $\text{CH}_3(\text{OCH}_2\text{CH}_2)_{13}\text{OCH}_3$ as a function of the mass fraction of the cyclic molecules (X_c). Although the average number of threading events is obviously maximized (1.73, 4.3%) when the system consists of 50% rings and 50% linear chains (not shown), Figure 1b

Threading Macro-crown Ether (MC-12). In order to identify the optimum size of macro-crown ether for threading, we first investigated the size and shape of simple crown ethers in the melt at



Scheme 1. Determination of Threading: (a) define local planes; (b) find the center of a local plane; (c) determine threading.

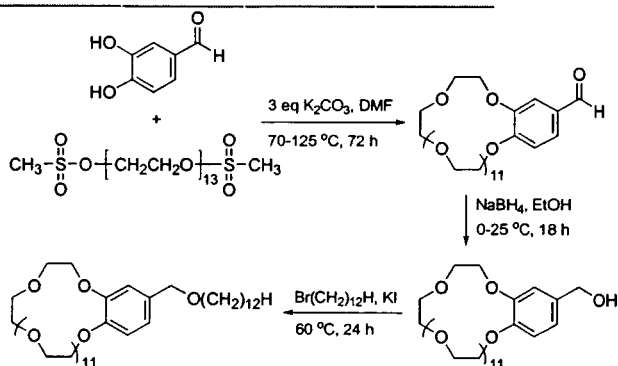
demonstrates that the *percentage* of rings threaded increases with decreasing concentration of those rings, with approximately 9% of rings threaded at high dilution of the cyclic component. The melt simulations also elucidated the location of 42-C-14 along the $\text{CH}_3(\text{OCH}_2\text{CH}_2)_{13}\text{OCH}_3$ linear chain in a system with $X_c = 0.5$. Although the cycle was twice as likely to be located at the end of the chain compared to the interior, it had equal probability of being located at any of the other interior locations, which demonstrates that the macrocrown ether is free to move along the linear PEO chain, or that the linear PEO chain is free to move through the macrocrown ether. While both types of motion occur, simulations suggest that the dominant mode in a laboratory-based coordinate system is slithering of the linear chain through the macrocycle, rather than shuttling of the macrocycle along the chain.⁵

Since our threading approach uses a solvent that selectively solvates the tail of the amphiphilic macrocrown ethers, we next simulated how the extent of threading 42-C-14 with $\text{CH}_3(\text{OCH}_2\text{CH}_2)_{13}\text{OCH}_3$ ($N_c = N_1$

Table 2. Mean-Square Radius of Gyration ($\langle R_g^2 \rangle$) of an Equal Number of $\text{CH}_3(\text{OCH}_2\text{CH}_2)_{13}\text{OCH}_3$ and 42-crown-14 at 373 K.

Volume fraction solvent	Solvent	$\langle R_g^2 \rangle_{\text{linear}}$ (\AA^2)	$\langle R_g^2 \rangle_{\text{ring}}$ (\AA^2)
0.00	None	47	28
0.75	Good	60	33
0.75	Θ	47	27
0.75	Poor	39	25

= 21 beads) is affected by diluting the melt with solvent, and by the solvent quality.⁶ The attractive pair-wise interactions of our good solvent bead and the polymer bead were three times stronger than those of two polymer beads in the melt, those of the poor solvent were one tenth weaker, and those of the theta solvent were equal. Table 2 summarizes the resulting $\langle R_g^2 \rangle$ values of $\text{CH}_3(\text{OCH}_2\text{CH}_2)_{13}\text{OCH}_3$ and 42-C-14 in the three solvents and in the melt. The simulations were consistent with established physical properties: $\langle R_g^2 \rangle_{\text{ring}} = 0.5 \langle R_g^2 \rangle_{\text{linear}}$; the



Scheme 2. Synthesis of "3,4-(42-crown-14)benzyl dodecyl ether" (MC-12).

radii in the melt were approximately equal to those under theta conditions; and the radii increased with increasing solvent quality. Figure 2a presents the extent of threading of 42-C-14 with $\text{CH}_3(\text{OCH}_2\text{CH}_2)_{13}\text{OCH}_3$ as a function of solvent content for systems with an equal number of rings and threads.

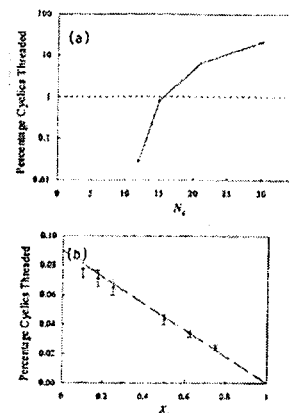


Figure 1. Percentage of cyclic molecules threaded as a function of (a) ring size N_c with $X_c = 0.25$ and $N_1 = 21$, and (b) the mass fraction of cycles (X_c) with $N_c = N_1 = 21$.

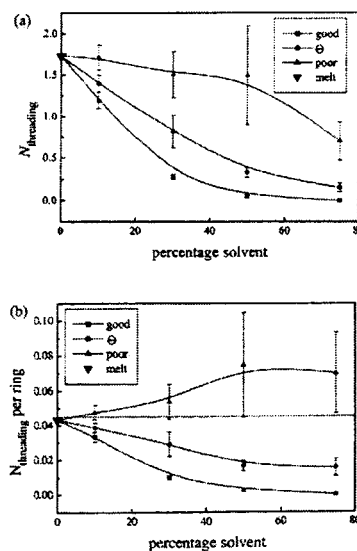
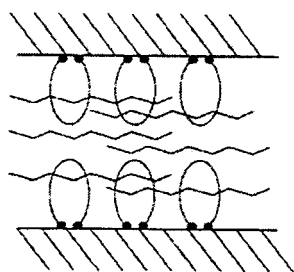


Figure 2. (a) Average number of 42-crown-14 cycles threaded with

Compared to the melt (1.73 threading events = 4.33% of the rings threaded), the number of threading events decreases with dilution since there are fewer rings present. Although the ring dimensions increase as the solvent quality increases, the extent of threading decreases. This indicates that threading is favored by aggregation in a poor solvent, which supports our amphiphilic threading approach. Figure 2b plots the corresponding number of threadings per ring, and demonstrates that the percentage of rings threaded are lower in the theta and good solvents than in the melt. Given the large error of the data in the poor solvent, we can only conclude that the percentage of rings threaded in the poor solvent are at least comparable to that in the melt, if not better, although these values are never greater than 10% threading.

Although we previously synthesized the amphiphilic analog of 42-C-14 (MC-12) in relatively high yield by the route shown Scheme 2,⁷ it produced not only the distribution of ring sizes corresponding to "monodisperse" PEG600 (600 Da), but also ~17% of the cyclic dimer after purification. We therefore repeated this synthesis and confirmed that the product of each step was pure by MALDI-ToF MS, in collaboration with Prof. Chrys Wesdimiotis, before proceeding to the next step.⁸ The most important step in the synthesis is the macrocyclization of PEG600-bismesylate⁹ with 3,4-dihydroxybenzaldehyde under pseudo-high dilution conditions¹⁰ in the presence of multiple potassium template ions.¹¹ According to MALDI-ToF MS, the crude product contained linear oligomers and cyclic dimer and trimer, in addition to the desired 3,4-(42-crown-14)benzaldehyde (MC-CHO). The cyclic oligomers were isolated from the linear oligomers by column chromatography using silica gel as the



Scheme 3. Threading simulations using modified beads that have attractive interactions with a surface.

Table 3. Threading of 42-C-14 with $\text{CH}_3(\text{OCH}_2\text{CH}_2)_{13}\text{OCH}_3$ at 373 K in a Confined Geometry.

Box Size (# sites)	Average Threading	Threading vs. Melt	% Rings Threaded
20x20x20	1.43	0.83	3.6
24x24x14	2.50	1.45	6.2
27x27x11	2.91	1.68	7.2
34x34x7	3.73	2.16	9.3

stationary phase and collecting the first fraction eluted with methanol/ CHCl_3 (5:4). The unimeric MC-CHO was isolated from the cyclic mixture by soxhlet extraction of the oils supported on a minimum amount of silica using hexanes, with the cyclic unimer extracted first. The remaining steps proceeded as outlined in Scheme 2.

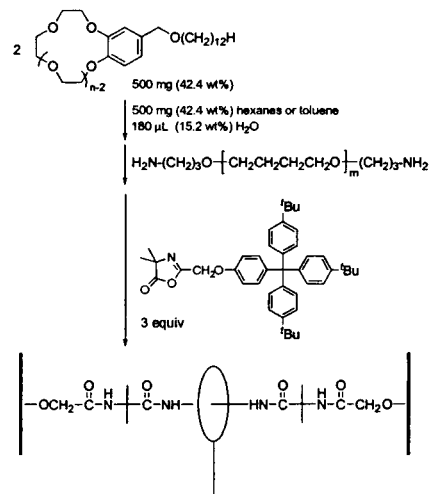
As demonstrated by X-ray diffraction and polarized optical microscopy, MC-12 organizes into a lyotropic lamellar (L_α) mesophase in hydrocarbon solvents if small amounts of water are added.^{7,12,13} In order to mimic this lamellar structure in simulations and determine its effect on threading, we added periodic boundary conditions to represent a solid surface and modified two consecutive beads per 42-C-14 ring to be attractive to that surface (Scheme 2).¹⁴ Table 3 summarizes the results of threading 42-C-14 with

$\text{CH}_3(\text{OCH}_2\text{CH}_2)_{13}\text{OCH}_3$ in an equimolar mixture of the two as a function of the box size (number of lattice sites); the z-direction represents the distance between the two solid surfaces, with seven lattice sites corresponding to 13.5 \AA^2 , or slightly more than twice the R_g of the rings. The extent of threading more than doubled from that of the purely statistical threading in the melt if the distance between the

two surfaces was approximately equal to the size of the rings; nevertheless, this still corresponds to only about 9% threading of the rings, which is consistent with our synthetic threading results.⁸

One of the most conclusive methods for positively identifying a threaded structure is characterization of a high molecular weight compound whose molecular weight and chemical composition correspond to the sum of a combination of the cyclic and linear components.

Our previous threading experiment attempted to characterize the product(s) of threading MC-12 with PEG3350-bisamine (3350 Da) in an organized solution by MALDI-FT MS, but the results were inconclusive;⁷ i.e. a high molecular weight compound was apparently present, but its molecular weight was too high to accurately identify. We therefore used pure MC-12 to synthesize a rotaxane composed of one MC-12 ring threaded with one end-capped poly(tetrahydrofuran) (PTHF, 350 Da) oligomer by equilibrating half an equivalent of the thread with an organized solution of MC-12, and end-capping the threads with excess azlactone (Scheme 4).⁸ Although the resulting rotaxane is not formally a *homorotaxane*, both components are aliphatic polyethers, and the use of a PTHF thread instead of PEO enabled differentiation of the molecular weight distributions of the ring and the thread in the



Scheme 4. Threading of an organized solution of MC-12 ring with bis(3-aminopropyl)-terminated poly(tetrahydrofuran)350.

mass spectra of the rotaxane (in collaboration with Prof. Chrys Wesdimiotis), and thereby enabled positive identification of the rotaxane. The expanded rotaxane region of the MALDI-ToF MS spectrum in Figure 3 shows five molecular weight distributions, with the components present in the highest concentrations separated by 72.1 Da, which is the molecular weight of one THF repeat unit. The five distributions therefore correspond to PTHF with 1-5 repeat units. The components within each of these five distributions are separated by 44.0 Da, which is the molecular weight of one EO repeat unit, with the 10-mer present in the highest concentration. The mass corresponds to one MC-12 ring threaded with one end-capped PTHF molecule plus sodium. However, the full spectra showed a low abundance of the rotaxane ions, and high abundances of unthreaded MC-12 and end-capped thread ions in the product isolated from the threading experiment. (Analysis by GPC was inconclusive because both the rotaxane and a one-to-one complex elute at the same retention volume.) MALDI-ToF and electrospray ionization quadrupole ion trap MS analyses of the rotaxane sample and mixtures of MC-12 and end-capped thread, including studies using varying laser intensities, comparisons of linear and reflectron analysis modes of

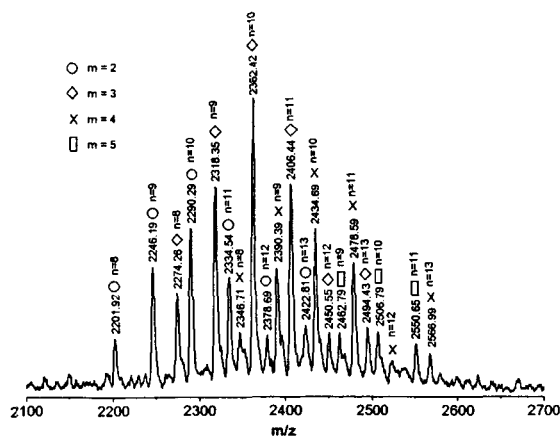


Figure 3. MALDI-ToF MS of the rotaxane from Scheme 6; mass = $1390.82 + (72.11)m + 290.44 + (44.05)n + 22.99$; m THF repeat units, n EO repeat units, dithranol as matrix, $\text{CF}_3\text{CO}_2\text{Na}^+$ salt, reflectron mode.

the ToF MS, and analysis of the rotaxane by the post source decay method demonstrated that the rotaxane does not fragment during the MALDI-ToF MS analysis, although the rotaxane ionizes less efficiently than either of its two components (C. Wedimiotis). We found that the rotaxane eluted separately from its cyclic and linear components by HPLC using silica columns and an eluant of THF with 0.3 wt% Aliquat 336 at 35 °C. The composition of the mixture qualitatively agreed with the MALDI-ToF mass spectrum, with 66 wt% end-capped thread, 23 wt% MC-12, and 11 wt% rotaxane. This yield is not sufficient to generate threaded structures in adequate quantities

to enable extensive characterization of the properties of (poly)rotaxanes. Therefore, we propose using columnar organization of the amphiphilic macrocycles to generate threaded structures; i.e. the MC-12 rings are evidently not optimally aligned within the L_α lyotropic lamellar mesophase, but should be aligned most effectively if they form a tube in a lyotropic columnar mesophase.

REFERENCES

- Helfer, C.A.; Xu, G.; Mattice, W.L.; Pugh, C., "Monte Carlo Simulations Investigating the Threading of Cyclic Poly(ethylene oxide) by Linear Chains in the Melt", *Macromolecules* **2003**, *36*, 9924-9928.
- Rapold, R.F.; Mattice, W.L., "New High-Coordination Lattice Model for Rotational Isomeric State Polymer Chains", *J. Chem. Soc., Faraday Trans.* **1995**, *91*, 2435-2441.
- Doruker, P.; Mattice, W.L., "Reverse Mapping of Coarse-Grained Polyethylene Chains from the Second Nearest Neighbor Diamond Lattice to an Atomistic Model in Continuous Space", *Macromolecules* **1997**, *30*, 5520-5526.
- Doruker, P.; Mattice, W.L., "A Second Generation of Mapping/Reverse Mapping of Coarse-Grained and Fully Atomistic Models in Polymer Melts", *Macromol. Theory Simul.* **1999**, *8*, 463-478.
- Rane, S.S.; Mattice, W.L., "Relative Magnitudes of the Short-Term Motions of the Cyclic and Linear Components of a Homorotaxane in Θ Media", *Macromolecules* **2004**, *37*, 7056-7060.
- Xu, G.; Rane, S.S.; Helfer, C.A.; Mattice, W.L.; C. Pugh, "Monte Carlo Simulation of Solvent Effects on the Threading of Poly(ethylene oxide)", *Modeling Simul. Mater. Sci. Eng.*, **12**, S59-S71 (2004).
- Pugh, C.; Bae, J.-Y.; Scott, J.R.; Wilkins, C.L., "An Amphiphilic Approach for Preparing Homopolyrotaxanes of Poly(ethylene oxide)", *Macromolecules* **1997**, *30*, 8139-8152.

-
8. Wollyung, K.M.; Xu, K.; Cochran, M.; Kasko, A.M.; Mattice, W.L.; Wesdemiotis, C.; Pugh, C., "Synthesis and Mass Spectrometry Studies of an Amphiphilic Polyether-Based Rotaxane that Lacks an Enthalpic Driving Force for Threading", *Macromolecules* **2005**, *38*, 2574-2586
 9. Crossland, R.K.; Servis, K.L., "Facile Synthesis of Methanesulfonate Esters", *J. Org. Chem.* **1970**, *55*, 3195-3196.
 10. (a) Jacobson, H.; Stockmayer, W.H., "Intramolecular Reaction in Polycondensations. I. The Theory of Linear Systems", *J. Chem. Phys.* **1950**, *18*, 1600-1606. (b) Jacobson, H.; Beckmann, C.O.; Stockmayer, W.H, "Intramolecular Reaction in Polycondensations. II. Ring-Chain Equilibrium in Polydecamethylene Adipate", *J. Chem. Phys.* **1950**, *18*, 1607-1612.
 11. Chenevert, R.; D'Astous, L., "Synthesis of Large Ring Crown Ethers", *J. Heterocyclic Chem.* **1986**, *23*, 1785-1787.
 12. Brandys, F.A.; Pugh, C. "Lyotropic Behavior of "3,4-(42-Crown-14)benzyl Dodecyl Ether" in Toluene in the Presence of Water", *Macromolecules* **1997**, *30*, 8153-8160.
 13. Pugh, C.; Bae, J.-Y.; Arehart, S.V.; Brandys, F., "Formation of Organized Structures through Variation in Molecular Architecture and Chemical Composition", *J. Macromol. Sci., Pure & Appl. Chem.* **1997**, *A34*, 2057-2071.
 14. Rane, S. S.; Mattice, W. L.; Pugh, C., "Modification of Statistical Threading in Two-Component Pseudorotaxane Melts Using the Amphiphilic Approach and Variations in the Confinement Geometry", *J. Chem. Phys.* **2004**, *120*, 10299-10306.